Research Article

Optimization of a Filament Wound Hybrid Metal Composite Railway Axle Design Concept

Guido Carra and Davide Formaggioni
Bercella S.R.L. 10 Via Enzo Ferrari, Varano de' Melegari, PR, Italy

Michael Sylvester Johnson and Preetum Jayantilal Mistry
Composites Research Group, Faculty of Engineering, University of Nottingham, Advanced Manufacturing Building, Jubilee Campus, United Kingdom

Andrea Bernasconi and Stefano Bruni*
Department of Mechanical Engineering, Politecnico di Milano, Milano, Italy

* Corresponding author. E-mail: stefano.bruni@polimi.it DOI: 10.14416/j.asep.2022.03.006
Received: 10 November 2021; Revised: 21 December 2021; Accepted: 3 February 2022; Published online: 21 March 2022

Abstract
This paper presents a numerical design method to develop a mass-minimized winding sequence for carbon fiber reinforced tubes to be manufactured by filament winding. This method combines the use of Altair Optistruct Finite Element Solver and CADWIND V9 CAM software to develop a winding sequence to implicitly compensate for the loss of stiffness due to fiber intertwining. Hence, it was specifically built to solve a stiffness-driven mass optimization design task of a hybrid metal composite railway axle, in which the design constraints were imposed by a previously developed design solution. However, in theory, it could be applied to the design of composite shafts for various applications.

Keywords: Railway axles, Carbon-fiber-reinforced polymer, Composites manufacturing, Filament winding, Roll wrapping, Composite materials

1 Introduction

A key consideration for the design of the railway wheelset of the future is mass reduction [1] and of particular focus is the mass associated with infrastructure damage [2].The cost of infrastructure maintenance and renewal already exceeds €25 billion a year across Europe, and this is continuing to rise. In this regard, reducing the mass of the wheelsets (i.e. the assembly comprising two wheels connected by an axle) is of paramount importance as these so-called un-sprung masses are directly in contact with the track. Hence, the wheelsets cause the most damage to the rails and other track components, due to the large shock forces and vibration. Recently, through the NEXTGEAR project [3] concepts for hybrid metal-composite (HMC) wheelsets have been proposed, with the aim of substantially reducing the un-sprung mass of the vehicle [4]–[6]. However, the concepts proposed so far have not explored the effect of the manufacturing process of the carbon-fiber-reinforced polymer (CFRP) tube as part of the design, and the contribution to the mass reduction that can be achieved.

The NEXTGEAR project, funded by the European Commission, aims to develop new technological concepts towards the next generation of railway rolling stock. This includes the development of a concept for an HMC axle as a part of a wheelset featuring substantial mass reduction as compared to a benchmark wheelset entirely made of steel [6]. As part of this research, the effect of the process to be adopted for manufacturing the tube, i.e. the composite section of

the axle, was investigated in detail. Two manufacturing methods were explored: roll wrapping (RW) and filament winding (FW). Although RW is better suited to minimize the overall composite mass by optimizing the direction of fibers, it is labor intensive and expensive. The process also introduces quality variability under mass production, which is highly undesirable for a safety critical component. FW, on the other hand, introduces some limitations on fiber orientation which inevitably result in an increase of the composite mass. However, it is an automated process offering the advantages of both cost reduction and quality improvement of the manufacturing process [7], [8]. This paper aims to propose a methodology defining a fiber layup pattern manufacturable by FW that minimizes the mass increase compared to a reference roll-wrapped solution whilst maintaining the same bending and torsional stiffness.

As the axle is mainly subjected to a 4-point rotating bending loading condition with predominant stresses in the axial direction, most of the plies should be axially oriented. Hence, the disadvantage of FW compared to RW stems from the inability to orient fibers axially. The mechanical properties of filament wound structures strongly depend on the winding pattern [9]. Process parameters, particularly tow tension applied during filament winding, can influence the physical and mechanical properties of the component [10]. Moreover, the FW process intrinsically generates an intertwining among tows being wound in different winding strokes. Consequently, local variations of ply thickness and orientation angle are produced within the laminate. These local variations are relatively limited, but their integration over the whole length might imply a reduction of the global stiffness that shall be quantified and compensated for in the design process. Finally, because of the particular way FW lays fibers, and as different winding patterns generate different extents of fiber overlapping, the thickness of each ply is influenced by the process itself.

Figure 1 shows the reference concept of the HMC railway axle [6]. This includes a full-length inner composite tube referred to as the primary tube PT (1), which is overwrapped in the central portion by an external composite secondary tube ST (2) to meet the bending stiffness requirements. Two metallic collars (3) are adhesively bonded at the ends of the axle, providing suitable interfaces to the wheels which

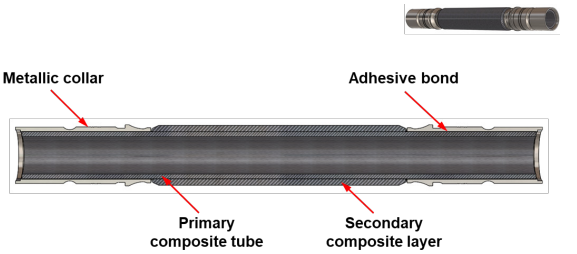

Figure 1: Hybrid Metal Composite concept axle.

are shrink-fitted to the axle. The components of this HMC axle under investigation in this work are the primary and secondary tubes.

2 Methodology for FW Optimisation

The methodology used to optimize the FW process is detailed in the flow chart shown in Figure 2.The initial step (1) is the analysis of the reference design, manufactured by RW, to define design requirements. Design constraints for the HMC railway axle are stiffness-driven and involve the maximum allowable deformations (displacements and rotations).

In the next step (2), a filament-wound layup of the PT and ST tubes having minimum mass is sought, while maintaining equal or reduced deflection and rotation as the roll-wrapped design under the same load and constraint condition. The software chosen to implement this optimization process is HyperWorks by Altair, containing the OptiStruct solver suite [11]. This allows for the numerical optimization of composite laminates both in terms of ply thickness and stacking sequence. In this step, the structure is modeled as a composite laminate, with a layup consisting of layers of unidirectional fibers having orientations that respect the manufacturing constraints of FW. Maximum allowable deflections are defined based on the analysis of the reference RW design and multiplied by knock-down factors accounting for the difference between the stiffness of a composite laminate and that of a filament wound structure.

In the next step (3), the CadWind Software [12] was used to simulate the FW process and define the local properties of the material. Taken into account was the interweaving of fibers and the non-uniform fiber orientation resulting from the combination of hoop and helical winding.

Then, two finite element models are defined:

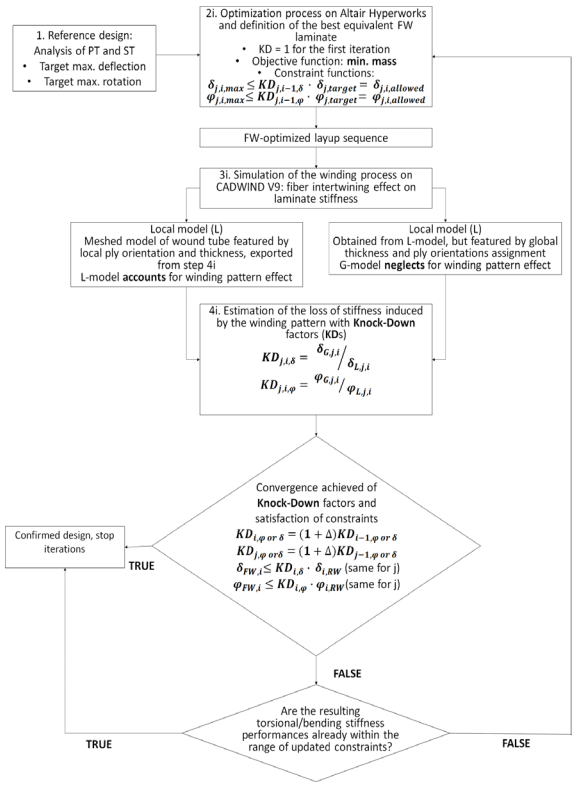

Figure 2: Filament winding stacking sequence development process flow chart.

one with local properties extracted from the CadWind result file (L), and one with the staking sequence provided by OptiStruct (G). The comparison of the results of these two analyses allows for the evaluation of the knockdown factors to be applied to the deformation constraints in Step 2 (step 4). These analyses were performed using the software Abaqus by Simulia.

At this point, the satisfaction of constraints is checked. If it is confirmed that the FW design is at least as stiff as the reference RW design the procedure stops, otherwise the values of the knockdown factors are updated and the procedure is iterated until convergence is reached. The steps are described in more details in the following subsections.

3 Analysis of the Reference Structure (Step 1)

The roll-wrapped primary (PT) and secondary tubes (ST) are analyzed separately. Considering the design of the HMC axle in Figure 1, it might appear more appropriate to analyze the assembly of the two tubes, instead. However, the choice of considering the PT and ST separately is dictated by the optimization solver used in Step 2, which assumes that the shell model corresponds to the middle surface of the laminate. This assumption can only be respected by considering the two tubes as separate entities. In fact, there is no means to know a priori where the final position of the interface between primary and secondary tubes will be at the end of the optimization process, hence the two tubes cannot be reduced to a single equivalent laminate. For these reasons, a final validation of the results is required in a separate and independent analysis, where the filament wound final design will be checked against the assembled roll-wrapped primary and secondary tubes.

The PT and ST are considered to be subject to 4-point bending and 3-point bending, respectively, plus torsion. Their maximum static transversal deflection δ and rotation φ are evaluated. The values obtained for the roll-wrapped PT and ST, denoted as $\delta_{PT,RW}$, $\delta_{ST,RW}$, $\varphi_{PT,RW}$ and $\varphi_{ST,RW}$ set the targets for the filament-wound design. The tubes are modeled as shell parts representing the mid surface. The laminate is meshed with linear, 4 nodes shell elements. The bogie loads and braking forces in the two transverse planes are derived from BS 8535-2011 and applied. The same load values will also be adopted for result validation.

The laminate definition is completed by assigning a ply-based property section to the whole shell model. For the simulations on roll wrapped tubes, Gurit UCHM 450 SE84 unidirectional prepreg lamina (0.45 mm thick) is used. In the presented case an orthotropic lamina material model is chosen. The stacking sequence for the primary tube is [90/±45/02/90/±45/90/02/±45/02]S, resulting in a 30-ply, 13.5 mm thick laminate. The same modeling options are considered for the secondary tube, with a different stacking sequence [(90/±45/04/±45/04/90/0]S. The ST is bound at its ends to the PT and comes in contact with the PT in the center of the axle when this latter tube bends due to the loads applied. The resulting loading condition for the ST can be simplified as a 3-point bending case. Using the above-described models and assumptions, the reference displacement $\delta_{PT,RW}$, $\delta_{ST,RW}$ and rotations $\varphi_{PT,RW}$, $\varphi_{ST,RW}$ are eventually determined and reported in Table 1.

Table 1: RW design primary and secondary tube stiffness indicators

Property	RW-Primary Tube (PT)	RW-Secondary Tube (ST)	Units
Stacking sequence	$[90/\pm45/0_2/90/\pm45/90/0_2/\pm45/0_2]_S$	$[(90/\pm45/0_4/\pm45/0_4/90/0]_S$	[--]
Max. transversal deflection	6.60	1.14	mm
Max. rotation	6.06	5.23	mrad
Min. rotation	–8.02	–3.57	mrad

4 Optimization of the FW Layup (step 2)

The second step (2) of the process shown in Figure 2 consists of the generation and optimization of a trial layup for filament winding. This is performed in Optistruct using a numerical optimization method. The starting point of the optimization process is the generation of an over-conservative layup, which is derived from the RW layup replacing plies at 0° with ones laid at ±10°. An excessively conservative initial guess does not jeopardize the outcomes of the optimization process since useless plies (providing a small contribution to the tubes' stiffness) are eliminated by the solver during the process. Thus, the initial number of plies is increased with respect to the RW layup, to make sure the optimization process starts from a feasible design respecting the constraints on stiffness.

The optimization process depends on some inputs, among which of crucial relevance are:

- Objective function: a quantity to be maximized or minimized according to the design requirements and which is dependent on the design variables. In the presented study, the mass of the PT and ST shall be minimized.
- Constraint functions: non-negotiable conditions that the result shall respect to be considered acceptable. These are:

$$\delta_{j,i,\max} \le KD_{j,i-1,\delta}\delta_{j,RW} = \delta_{j,i,allowed}$$
$$\varphi_{j,i,\max} \le KD_{j,i-1,\varphi}\varphi_{j,RW} = \varphi_{j,i,allowed}$$

Where:

i = iteration counter;

j = primary (PT) or secondary (ST) tube;

$\delta_{j,i,\max}$ = max. transversal deflection of the filament-wound PT or ST (i-th iteration);

$\varphi_{j,i,\max}$ = max. rotation about the axis of the filament-wound PT or ST (i-th iteration);

$KD_{j,i-1,\delta}$ = Knock-Down factor for bending stiffness due to fiber intertwining for the PT or ST identified at the previous iteration;

$KD_{j,i-1,\varphi}$ = Knock-Down factor for torsional stiffness due to fiber intertwining for the PT or ST identified at the previous iteration;

$\delta_{j,i,allowed}$ = max. allowed value of transverse deflection adopted as an optimization constraint during the i-th iteration for the PT or ST

$\varphi_{j,i,allowed}$ = max. allowed value of rotation adopted as an optimization constraint during the i-th iteration for the PT or ST

Knock-Down factors (KD) are introduced to account for the reduction of the bending stiffness of the PT and ST due to fiber intertwining and their values are expected to be between 0 and 1. This means fiber intertwining is assumed to be detrimental or, in the best case, neutral to the stiffness of the laminates. The values of the knock-down factors are set to 1 for the zero iteration, i.e. the winding pattern is initially assumed to have no influence on laminate stiffness, and are updated once the process simulation is performed at Step 3 and a model accounting for the true fiber orientation on the FW structure is built.

The initial guess must belong to the feasible design space. Hence, plies at 0° are re-oriented to ±10°, and the number of plies is increased.

- PT layup guess:

$[(90/\pm45/\pm10/90/\pm45/90/\pm10/\pm45/\pm10)_2/(90/\pm45/\pm10_2/\pm45/\pm10_2/90/10)_2]_S$ (120 plies)

- ST layup guess:

$[(90/\pm45/\pm10/90/\pm45/90/\pm10/\pm45/\pm10)_2/(90/\pm45/\pm10_2/\pm45/\pm10_2/90/10)_2]_S$ (120 plies)

The choice of maintaining nearly axial, hoop and 45°-inclined plies only is motivated by the analysis of the design problem. This primarily involved with ensuring the desired bending and torsional stiffness for the axle: bending stiffness is provided by plies at ±10°, torsional stiffness is mainly provided by 45° plies and finally 90° plies contribute to prevent delamination in case of local fibers breakage. The shell models of filament-wound PT and ST are defined using the same assumptions and loads as for the RW ones.

OptiStruct completes the required task with a three-step numerical process that prevents the use of a trial-and-error approach.

Free-size optimization: combines topology and

topography optimization of meshed shells with defined initial stacking sequence. The solver also provides the possibility to account for manufacturing constraints such as minimum ply thickness and pairing of opposite angle plies to ensure a balanced output stacking sequence. A cluster of elements constrained to have the same thickness within each ply shall be set over the whole shell model, to prevent the solver from generating intricately shaped patches neither compatible with roll wrapping nor with filament winding. This first phase also establishes which plies among the ones of the overconservative initial guesses contribute the most to stiffness. It preserves the initial stacking sequence but sets each single ply thickness to the minimum allowed value and, consequently, it allows for a preliminary analysis of the laminates. According to the scope of the design process, the mass of the laminate is set as the objective function and the maximum deflection and rotation values are extracted to check that optimization constraints are met. Each single ply thickness, conversely, shall be set as a design variable. The free-size optimization is exemplified for the PT, while the same process is also performed for the ST. First, design responses are required by the solver: laminate mass (MASS_RESP), maximum rotation (ROT_EDGES) and displacement (DISP_RESP). These latter two quantities shall be extracted in those nodes where their maximum values are expected to be observed.

Then, responses of interest are checked against a condition of acceptability:

- DISP_RESP < $KD_{PT,i-1,\delta}\delta_{PT,RW}$
- ROT_EDGES < $KD_{PT,i-1,\varphi}\varphi_{PT,RW}$

With the values of the KDs being equal to one for the first iteration. Regarding the objective function, the quantity to be minimized is the overall mass of the PT. The output result preserves the same stacking sequence as the overconservative initial guess, but strongly reduces ply thickness. According to the rationale of this first optimization run, the contribution given by each single ply to the overall laminate stiffness is directly indexed by their thickness. Plies contributing the most are the ±10° and ±45° ones as they are featured by the largest thickness (in the order of tenths of a mm). Conversely, plies at 90° are almost non-contributing.

At the end of the iterations, the solver proposes a final solution for the PT and the ST characterized by the values of laminate thickness and mass reported in Table 2. The values of the final design responses (rotation, deflection) are very close to the limit values imposed by the design constraints. The optimization process, indeed, can be judged as efficient since the minimum quantity of material needed to ensure the acceptability of the solution is found. This is enabled by the small number of constraints prescribed and by the possibility to assign plies with arbitrary thicknesses values (which may lead to manufacturing issues). As the optimization becomes more bounded, the final mass of the laminates and the gap between the response of the final design value and the constraints might become larger.

Table 2: Free-size optimization results for PT and ST

Free-size Optimization: Results	Primary Tube (PT)	Secondary Tube (ST)	Units
Laminate thickness	18.01	13.25	mm
Laminate mass	16.83	8.12	kg
N. of plies	120	120	-
Min. ply thickness	0.004	0.1	mm
Orientation of min.-thickness ply	90°	90°	-
Max. transversal deflection (abs.)	6.45	0.97	mm
Max. rotation (abs.)	5.97	4.93	mrad

Ply-bundle optimization: this second optimization step allows for a refinement of the previously obtained design. The solver is asked to optimize the mass of the laminate by deciding whether each ply should be assigned with a manufacturable thickness or should be removed. The definition of a minimum manufacturable thickness involves the discretization of the domain of output masses for the optimized solution. The results obtained at the end of this step are presented in Table 3. The laminates now include a smaller number of plies, each 0.3 mm thick, which means in the optimization the minimum feasible thickness is assigned to each one of the plies. The PT preserves only 78 plies out of the initial 120 plies, whereas the ST preserves 48 plies. From a quick comparison among results in Tables 2 and 3, it can be observed that the refining step causes a significant mass increment for both the PT and the ST which is due to the additional bounds on manufacturable thicknesses imposed to the solver. Consistently, the maximum displacements and rotations found after the ply-bundle optimization is performed are much lower

than the maximum allowed values. Overall, the solver determined that the thickness of plies should be smaller than the minimum allowed value of 0.3 mm, which would lead to deflection and rotation outputs close to the limiting values and would enable a reduction of the mass. However, the constraint on ply thickness forces the optimization to a different value in the space of feasible designs. The smaller the difference between the imposed minimum manufacturable ply thickness and the thickness values resulting from the free-size optimization, the smaller the mass increase at the end of the ply-bundle optimization. Therefore, the results of the ply-bundle optimization can be pushed toward further reduced masses by allowing a lower minimum thickness of the plies.

Table 3: Ply-bundle optimization results

Ply-bundle Optimization: Results	Primary Tube (PT)	Secondary Tube (ST)	Units
Laminate thickness	23.40	14.40	mm
Laminate mass	21.83	8.88	kg

Ply-shuffle optimization: this is a non-mass optimizing step. During this last optimization step, the solver shuffles the order of plies to increase the gap with respect to the bounds given by design constraints. The designer can specify the maximum number of adjacent plies having the same orientation and it is possible to forbid the solver to separate plies having defined orientations during the last optimization step. As filament winding lays fibers in opposite directions in the front and back strokes, these settings were applied to all the plies having a nominal orientation of 10° and 45° respectively. The solver terminates the iterations on the ply stack when two consequent iteration sequences provide an identical result, no matter if it behaves better than the original laminate or not in terms of overall bending and torsional stiffness. In this case, where the results proposed by the solver for both primary and secondary tubes did not improve the solution obtained after ply-bundle optimization. Consequently, the outcome of the ply-bundle optimization step was considered instead as a reference result for the current iteration.

The minimum ply thickness is an important parameter used by the solver to discretize the domain of the thicknesses that can be assigned to a ply. Thus, the solver can assign thicknesses being integer

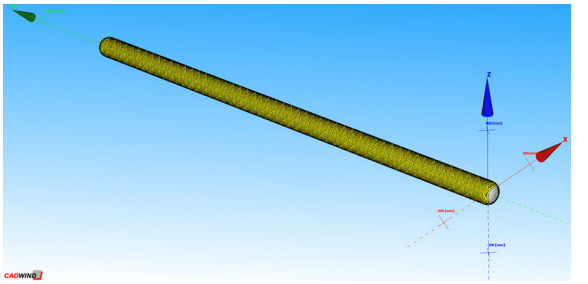

Figure 3: Trial winding process simulation to determine ply-thickness (45°).

multiples of a minimum one. In the case of filament winding, these thicknesses are orientation-dependent: different deposition angles carry out a slightly different thickness for each ply. The CadWind software is used to determine these ply thicknesses by simulating the winding process over the mandrel. Material properties were input as listed in the manufacturer's datasheet:

- Towpreg impregnated in a fire-retardant resin
- Single roving winding
- 6 mm wide tape, 24 K carbon fibers
- 67% fiber mass content, 1600 tex.

Plies at ±10° and ±45° (Figure 3) result in a minimum thickness of 0.296 mm whilst hoop-wound plies have a minimum thickness of 0.302 mm. To ease the implementation of the optimization software, the derived thicknesses are rounded to 0.300 mm.

After the data is captured, the optimization algorithm can be executed. Upon process convergence, a trial filament winding layup is generated. The trial stacking sequence mostly depends on the values of constraint functions, and, therefore on the KD factors that shall be estimated. To quantify them, an additional function of CadWind Software is used, which allows for the simulation of the whole winding process by superposing the layers of the trial layup sequence (Step 3). It also enables the extraction of a meshed shell model accounting for the local thickness and material orientation variations due to fibers intertwining, and causing the mentioned losses of global stiffness, which ultimately leads to the evaluation of the KD factors.

5 Simulation of the Winding Process (step 3)

Simulation of the winding process and the extraction of meshed shell models representing the laminates are the chosen means to introduce the effect of the winding

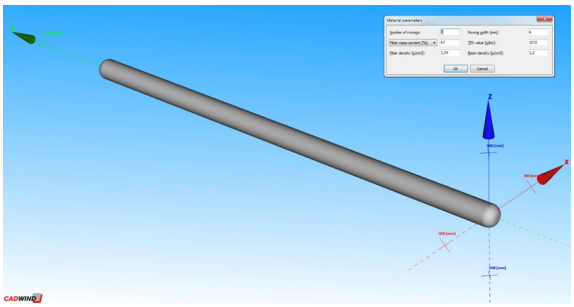

Figure 4: CADWIND mandrel viewport and material properties input.

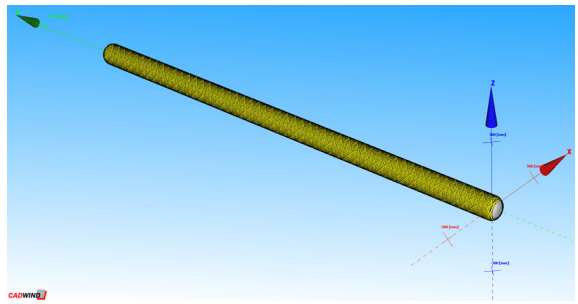

Figure 5: Non-geodesic winding for 45° fiber orientation.

pattern on the overall laminated tubes stiffness. These latter models account for the local variations of thickness and material orientations due to the intertwining of fibers. These simulations are performed using the CADWIND software.

The mandrel geometry (Figure 4) is designed to facilitate not only the simulation of the winding process but also to be representative of the possible winding process of the tubes as well. Therefore, a cylindrical mandrel with hemispherical ends and cylindrical bosses (connecting the mandrel to the spindle of the winding machine and the opposite support) is designed.

Although the dimensions of the mandrel could be arbitrarily assigned, a slender geometry is chosen for the mandrel: the nominal diameter is set to the internal collar diameter equal to 142 mm, whilst the length is set to 2400 mm. This choice is dictated by the need to determine the effect of the pattern on the bending stiffness: in fact, the slenderer the laminate is, the more negligible the contribution of shear deformation to the maximum transverse deflection will be. Conversely, this would have no influence on torsional stiffness under axially oriented torque. The adopted tow properties are referred to as the fiber tows pre-impregnated in an epoxy resin (CTP24/6-5.0/270-E910/33%). Results of the simulation are illustrated in Figure 5 and reported in Table 4, where it is shown that none of the wound layers are generated with the traditional winding processes (circumferential, helical, polar) but a non-geodesic winding is chosen instead.

Geodesic paths describe the shortest fiber path connecting two points over the mandrel surface; indeed, the helical winding is a geodesic winding. A non-geodesic winding, therefore, is a fiber path calculation method that does not generate an optimal path, but it is a versatile way of covering the mandrel that takes advantage of the friction among tows and the surface underneath to close patterns that do not pass right beside the bosses connected to the spindle. For this reason, a friction coefficient, here assumed as equal to 0.2, shall be defined. The laminate thus obtained is exported for both PT and ST into files whose format allows for data to be imported by different FE modelers (Abaqus CAE included).

Table 4: Winding parameters adopted for winding simulation

Free-size Optimization: Results	**Ply ≈90**	**Ply 45**	**Ply 10**
Type of winding	Non-geodesic	Non-geodesic	Non-geodesic
Deg. of covering	105%	105%	105%
Pattern number	1/1	7/6	9/8
No. of layers	1	1	1
Dwell front	90°	90°	90°
Dwell back	90°	90°	90°
Ply thickness	0.30 mm	0.29 mm	0.30 mm

The input for CADWIND is the staking sequence defined by the Optistruct solver at the previous step. Slight modifications have been operated on both the PT and ST stacking sequences. Despite the optimization process eliminating the hoop-wound fibers that were included in the most internal and external layers of both PT and ST tubes, they are re-introduced because:

- Plies at 90°, with fiber pre-tension, provide a relevant contribution to the robustness of the laminate tubes thanks to the imposition of radial stress; in fact, in case impact protection is ineffective and local

fiber breakage occurs, hoop wound layers (if intact) would contribute to keeping fibers in place preventing catastrophic failures due to sudden delamination;

- Plies at 90° are also relevant for the fitting of the collars onto the laminate tube, as they withstand most of the imposed radial stress.

6 Knock Down Factors Estimation (step 4)

The strategy to estimate the KD factors is to compare the performances of the model exported from CadWind with another being identical in terms of geometry, mesh type and size, and loading conditions but with uniform thickness and layer-wise material orientation assignments:

$$KD_{j,i,\delta} = \delta_{G,j,i} / \delta_{L,j,i}$$
$$KD_{j,i,\varphi} = \varphi_{G,j,i} / \varphi_{L,j,i}$$

Where:

$\delta_{L,j,i}$ = max. vertical displacement of the "local" PT or ST model (i-th iteration);

$\delta_{G,j,i}$ = max. vertical displacement of the "global" PT or ST model (i-th iteration) ;

$\varphi_{L,j,i}$ = max. rotation about the axis of the "local" PT or ST model (i-th iteration) ;

$\varphi_{G,j,i}$ = max. rotation about the axis of the "global" PT or ST model (i-th iteration).

Pattern effect is defined as the consequences of all the local variations of winding angle, that are relatively small but, if enveloped over the whole laminate, may carry out relevant losses in terms of bending and torsional stiffness. The evaluation of such effect is performed using a comparison of the FE shell models exported from CADWIND, that are featured by the mentioned orientation variations (local model), with others being identical in terms of geometry, stacking sequence and load condition but featured by a layer-wise material orientation assignment, with layers of uniform properties (global model). The knockdown factors are eventually calculated as the ratios among the performances of the local and the global models separately for the PT and the ST, as these effects are assumed to be stacking-sequence dependent. The estimation process is reported for the PT stacking sequence only, and it is repeated for the ST one.

6.1 *Analysis of the local model*

The FE model exported from CADWIND is imported in a new Abaqus CAE session and a new model with an orphan mesh is generated. To define elastic properties, the laminate is sliced into several transverse sections and to each of these sections, a different stacking sequence is assigned. Each ply generated by a certain winding cycle is split into two different layers having opposite angles. Consequently, from 78 plies each 0.3 mm thick, a stack of 156 plies each nominally 0.15 mm thick is obtained. The shell model is subdivided in a series of transverse sections and to each of the obtained partitions a Shell, Composite section is assigned.

Subsequently, a static, general step is generated. Three-point bending, and an axial torque are applied to the laminate, and it is then constrained so that it behaves as a simply supported beam. The results for the local model of the primary tube stacking sequence (i.e. the wound laminate having the same stacking sequence as the one of the primary tubes and accounting for the winding pattern effect) are then obtained. of this example.

6.2 *Analysis of the global model*

The global model is identical to the local model apart from the material assignment, which is assigned by defining a stacking sequence to a shell model in Abaqus CAE by means of the Composite Layup Tool. All other model features including geometry, mesh, material properties, loads, constraints and mesh are left unvaried. Therefore, once the material model has been set up, results of the simulation on the global model can be obtained. Values of the Knock-Down factors thus obtained are reported in Table 5.

Table 5: Winding pattern effect evaluation: Knock Down factors (KD)

Tube	"Global" Model Value UM	"Local" Model Value UM	KD
PT	28.72	28.43	>1
	0.058	0.060	0.967
ST	35.61	34.39	>1
	0.1391	0.1268	>1

It can be observed that 3 out of the total 4 KD coefficients are larger than 1: this means that, according

to the analysis performed, the effect of the winding pattern slightly increases the bending stiffness of the laminate, instead of being detrimental to it. To keep a conservative approach, all KD factors are saturated to 1. The single KD factor taking a value below 1 is $KD_{PT,\varphi}$. The value of this coefficient is so close to 1 that even considering the corresponding reduction of the PT stiffness the constraint on the rotational stiffness of the PT is still met.

Since the rotation of the lastly formulated stacking sequence of the primary tube already falls within the allowed range by the updated constraints, an additional iterative step would not produce any mass variation and the stacking sequence would not change as well. The same can be said for all of the other constraints since their values are not updated (KD = 1). Therefore, the iterative process can be stopped, and the stacking sequences formulated during the first iteration are the final ones.

7 Filament Winding-Optimized Stacking Sequence

After evaluating the KD factors, step 2 is repeated with the updated values of the KD factors and a new iteration is performed. The optimization procedure (step 8 of the iterative process depicted in Figure 2) ends whenever two subsequent iterations provide the same winding and therefore the same KD factors. Therefore, iterations are terminated whenever, assuming a certain tolerance, two subsequent iterations generate the same KD factors. It must be pointed out that in Step 2, the Optistruct analysis minimizes the mass of the tubes for the given KD factors. Therefore, the minimum mass problem is solved implicitly, nested into the iterative procedure that updates the KD factors. The final results of the FW optimization process are reported in Table 6.

Table 6: Filament winding stacking sequence optimization results

FW-Layup Optimization Results	Primary Tube (PT)	Secondary Tube (ST)	Units
Laminate thickness	23.40	14.40	mm
Laminate mass	21.83	8.88	kg
Stacking sequence	$90/\pm45_2/(\pm10/\pm45)_7/\pm45_3]_s$	$[90_2/\pm45_4/\pm10_7]_s$	[-]
Maximum deflection	4.81	0.95	mm
Maximum rotation	3.68	3.35	mrad

The masses of the PT and ST in the optimized FW design should be compared to 13.7 kg and 8.3 kg respectively for the RW design. Despite the relative mass increase of the optimized FW design compared to the RW design is approximately 60%, the absolute value of the total mass increase is less than 9 kg, which means most of the mass saving obtained by replacing the original steel axle with the HMC is still preserved. Furthermore, the analysis of FEA static cases showed that, compared to the RW design, the optimized FW design provides a reduction of the transversal stresses in the range of –10%, a reduction of the torsional rotation by more than 25% and a reduction of the maximum stress in the composite material by nearly 7%.

8 Conclusions

A methodology to optimize the filament winding manufacturing process for a hybrid metal-composite (HMC) railway axle is proposed in this paper. The method aims to minimize the mass of the composite axle, while meeting the bending and torsional stiffness requirements. This methodology considers the bespoke design of the HMC axle developed during the NEXTGEAR project, consisting of a primary tube coaxial with a secondary composite tube which is added to meet the requirements of the axle bending stiffness. The results obtained show that the minimization methodology, though being iterative in nature, converges quickly to a solution. In the case considered here, only one iteration of the procedure was actually required to obtain the solution. The results also show that the increase of the axle mass implied by the use of filament winding in place of roll wrapping is highly sensitive to the minimum thickness assumed for the plies. This, in turn, depends on the parameters of the FW process and the used material. Considering a minimum thickness of the plies of 0.3 mm the total mass increase is approximately 9 kg for the entire composite portion of the axle, consisting of the PT and ST. This is a significant proportion of the total mass of the composite parts but is quite small compared to the mass saving obtained replacing the steel axle with the HMC axle. Therefore, the use of FW in place of RW can still be justified, considering the benefits offered by FW in terms of repeatability of the manufacturing process, quality of the final product and total manufacturing costs.

Acknowledgments

This work was conducted as part of Work Package 3 of the NEXTGEAR Project, S2R-OC-IP1-02-2019 [Grant number: 881803], which is ascribed under the Shift2Rail Program funded by the EU Horizon 2020 research and innovation programme. The authors acknowledge the information regarding the benchmark inboard bearing, hollow steel axle provided by Lucchini RS, Italy. The fourth author would like to acknowledge the funding support of the Engineering and Physical Sciences Research Council through the: EPSRC Future Composites Manufacturing Research Hub [Grant number: EP/P006701/1] and EPSRC Industrial Doctorate Centre in Composites Manufacture [Grant number: EP/L015102/1].

References

[1] J.-P. Loubinoux and L. Lochman "Moving towards sustainable mobility: A strategy for 2030 and beyond for the European railway sector," presented at the International Union of Railways (UIC), Paris, France, 2012.

[2] S. Iwnicki, M. Spiryagin, C. Cole, and T. McSweeney, *Handbook of Railway Vehicle Dynamics*, 2nd ed. Boca Raton, Florida: CRC Press, 2019.

[3] NEXTGEAR, "NEXTGEAR Project," 2020. [Online]. Available: https://nextgear-project.eu/home.aspx

[4] J. Batchelor, "Use of fibre reinforced composites in modern railway vehicles," *Materials and Design*, vol. 2, pp. 172–182, 1981.

[5] P. J. Mistry and M. S. Johnson "Lightweighting of railway axles for the reduction of unsprung mass and track access charges," *Proceedings of the Institution of Mechanical Engineers, Part F: Journal of Rail and Rapid Transit*, vol. 234, pp. 958–968, Sep. 2019.

[6] P. J. Mistry, M. S. Johnson, S. Li, S. Bruni, and A. Bernasconi, "Parametric sizing study for the design of a lightweight composite railway axle," *Composite Structures*, vol. 267, 2021, Art. no. 113851.

[7] E. J. Barbero, *Introduction to Composite Materials Design*. Boca Raton, Florida: CRC Press, 2017.

[8] B. T. Åström, *Manufacturing of Polymer Composites*. Boca Raton, Florida: CRC Press, 2018.

[9] T. V. Lisbôa, J. H. S. Almeida, I. H. Dalibor, A. Spickenheuer, R. J. Marczak, and S. C. Amico, "The role of winding pattern on filament wound composite cylinders under radial compression," *Polymer Composites*, vol. 41, pp. 2446–2454, 2020.

[10] P. Mertiny and F. Ellyin, "Influence of the filament winding tension on physical and mechanical properties of reinforced composites," *Composites Part A: Applied Science and Manufacturing*, vol. 33, pp. 1615–1622, 2002.

[11] *Altair OptiStruct 2019 User Guide*, Altair Engineering, Troy, Michigan, 2019

[12] *CADWIND v9 User Manual*, SA Materials, Brussels, Belgium, 2014.